ACCSCIENCE PUBLISHING

Advanced Neurology

ORIGINAL RESEARCH ARTICLE

Emx1-Cre-mediated inactivation of PDK1 prevents plaque deposition in an Alzheimer's disease-like mouse model

Xiaolian Ye[1], Liyang Yao[2], Wenhao Chen[3], Wenkai Shao[2], Yimin Hu[3]*, Bing Zhang[1]*, and Guiquan Chen[2]*

[1]Department of Radiology, Medical Imaging Center, The Affiliated Drum Tower Hospital of Nanjing University Medical School, Institute of Medical Imaging and Artificial Intelligence, Jiangsu Key Laboratory of Molecular Medicine, Institute of Brain Science, Nanjing University, Nanjing, Jiangsu Province, 210008, China

[2]Model Animal Research Center, Department of Neurology, The Affiliated Drum Tower Hospital of Nanjing University Medical School, Jiangsu Key Laboratory of Molecular Medicine, Nanjing University, 12 Xuefu Avenue, Nanjing, Jiangsu Province, 210061, China

[3]Department of Anesthesiology, The Second Affiliated Changzhou People's Hospital of Nanjing Medical University, Changzhou, Jiangsu, 213000, China

Abstract

BX912, an inhibitor for 3-phosphoinositide-dependent protein kinase 1 (PDK1), has been shown to produce beneficial effects in mouse models of Alzheimer's disease (AD). To test the hypothesis that early inhibition on PDK1 may prevent neuropathology in a 5×FAD mouse model, we employed a genetic approach to generate a mutant line, termed as *Pdk1* cKO/5×FAD, in which PDK1 is inactivated, specifically in the developing cortex of 5×FAD mice through *Emx1-Cre*-mediated gene recombination. We discovered that the *Pdk1* cKO/5×FAD mice exhibited a massive reduction of plaque pathology compared with their 5×FAD littermates. We also demonstrated that gliosis was remarkably attenuated in *Pdk1* cKO/5×FAD cortices and amyloid precursor protein levels were significantly lower in *Pdk1* cKO/5×FAD cortices compared with 5×FAD littermates. This study suggests that early inhibition on PDK1 may effectively prevent AD-like neuropathology.

Keywords: Alzheimer's disease; Plaque deposition; PDK1; Neuroinflammation; Amyloid precursor protein; Conditional knockout

***Corresponding authors:**
Yimin Hu (guyueym@njmu.edu.cn)
Bing Zhang (zhangbing_nanjing@nju.edu.cn)
Guiquan Chen (chenguiquan@nju.edu.cn)

Citation: Ye X, Yao L, Chen W, *et al*., 2022, *Emx1-Cre*-mediated inactivation of PDK1 prevents plaque deposition in an Alzheimer's disease-like mouse model. *Adv Neuro*, 1(3): 153. https://doi.org/10.36922/an.v1i3.153

Received: July 9, 2022

Accepted: October 17, 2022

Published Online: November 30, 2022

1. Introduction

Alzheimer's disease (AD) is the most common type of dementia in the elderly. The typical pathological hallmarks include extracellular amyloid β-protein (Aβ) deposition, intracellular tangles formed by phosphorylated tau, and gliosis[1-3]. The mechanisms underlying AD pathogenesis remain to be determined. A number of factors, including Aβ[4,5] and tau[6], have been identified as important factors for the etiology of AD. It is believed that Aβ accumulation may induce inflammation and cause neuronal death in the brain[5]. Many studies have demonstrated that Aβ is a major target for the treatment of AD[7-12].

3-phosphoinositide-dependent protein kinase 1 (PDK1) is a well-known member in the phosphoinositide 3 kinase (PI3K) pathway. The PI3K signaling pathway has important physiological roles, including cell proliferation, cell metabolism, angiogenesis, and so on[13-21]. Evidence has suggested that PDK1 may be involved in AD. First, it has been shown that AD patients exhibit enhanced PDK1 activity in the brain compared with control subjects without AD[22,23]. Second, a recent transcriptomic study demonstrated a significant increase in *PDK1* mRNA levels in excitatory neurons in the prefrontal cortex of AD patients compared with control subjects[24]. Third, it has been found that PDK1 activity is enhanced in several lines of amyloid precursor protein (APP) transgenic (Tg) mice, including Tg2576, APP/presenilin-1 (PS1), and 3×Tg-AD mice[22,25,26]. Moreover, previous evidence has shown that BX912, a potent PDK1 inhibitor, significantly diminishes amyloid plaques and improves spatial memory in mouse models of AD[22], raising a possibility that PDK1 may serve as a therapeutic target for AD.

Pietri *et al.* explored the mechanisms underlying BX912-induced beneficial effects in mouse models of AD. They found that BX912 increases the activity of α-secretase through tumor necrosis factor-α-converting enzyme (TACE), promotes the trans-localization of TACE into the plasma membrane, restores α-secretase-dependent cleavage of APP, and attenuates Aβ-induced neurotoxicity[22]. The study suggests that the inhibition of PDK1 may be effective in halting AD. However, serious side effects have been reported from the inhibition of PDK1 pharmacologically or genetically. First, long-term treatment with BX912 results in the death of adult APP Tg mice[22]. Second, a straight knockout (KO) of PDK1 causes embryonic lethality in mice[27]. Third, neural progenitor cell (NPC)-specific inactivation of PDK1 results in apoptosis of cortical neurons and impairs spatial learning in mice[28]. Fourth, interneuron- or oligodendrocyte-specific deletion of PDK1 or its substrate Akt leads to postnatal death in mice before the age of day 21 (P21)[15,16,29].

In response to the findings of Pietri *et al.*, we propose that early inhibition of PDK1 function may prevent AD-like pathology in APP Tg mice. To test this hypothesis, we employed a genetic strategy to inactivate PDK1 in the developing cortices of 5×FAD mice. The latter, which have been widely used in the field of AD, are known to express five mutations on human *APP* and *PS1* genes[30]. It has been reported that plaque pathology begins to become apparent in the cortex and the subiculum in 5×FAD mice at 2 months[30]. On the other hand, Cre is known to be expressed mainly in NPCs in the developing cortex and in excitatory neurons in the postnatal forebrain of *Emx1-Cre* mice[31-34]. In this study, *Emx1-Cre* mice were bred with 5×FAD (*APP/PS1*)[30,35,36] and floxed *Pdk1*$^{f/f}$[28,37-39] to generate *Pdk1*$^{f/f}$*;Emx1-Cre;APP/PS1* mice, termed as *Pdk1* cKO/5×FAD hereafter. Amyloid plaques were hardly detected in *Pdk1* cKO/5×FAD cortices, and the population of ionized calcium-binding adaptor molecule 1 (Iba1)+ cells decreased significantly. Furthermore, there was a significant decrease in APP levels in *Pdk1* cKO/5×FAD mice compared with their 5×FAD littermates. The above findings support the notion that early inhibition of PDK1 may effectively prevent AD-like pathology.

2. Materials and methods

2.1. Mice

The mouse work was performed in accordance with the Guide for the Care and Use of Laboratory Animals of Nanjing University. The background strain for male and female mice was C57BL/6. All mouse lines, including *Pdk1*$^{f/f}$, *Emx1-Cre*, and 5×FAD mice, are described in our previous studies[15,28,33,35,37]. The mice were maintained in an animal facility at the Model Animal Research Center of Nanjing University. They were group-housed in a room without specific pathogens. The room temperature was maintained at 25 ± 1°C, and the mice had unrestricted access to food and water. The animal protocol (AP) for this study was approved by the Institutional Animal Care and Use Committee (IACUC) of Nanjing University.

The following primers were used for genotyping: Primers for floxed *Pdk1* were TGTGCTTGGTGGATATTGAT (forward) and AAGGAGGAGAGGAGGAATGT (reverse); primers for human *APP* were AGGACTGACCACTCGACCAG (forward) and CGGGGGTCTAGTTCTGCAT (reverse); primers for human *PS1* were AATAGA GAACGGCAGGAGCA (forward) and GCCATGAGGGCACTAATCAT (reverse); and primers for *Cre* were GCCTGCATTACCGGTCGATGCAACGA (forward) and GTGGCAGATGGCGCGGCAACACCATT (reverse).

2.2. Tissue preparation for biochemical and morphological studies

The mice were perfused with cold phosphate-buffered solution (PBS)[40]. The brain was cut sagittally into two hemispheres, in which the cortex was dissected from one hemisphere to prepare protein samples. The other hemisphere was fixed in 4% paraformaldehyde (PFA) (Aladdin Biochemical Technology, C104188) at 4°C overnight and then dehydrated using a series of ethanol solutions (Nanjing Reagent, C0691510225). The dehydrated brain hemispheres were embedded in a paraffin machine (Leica Biosystems, 39601095) for the preparation

of paraffin blocks. There were four brain hemispheres in each paraffin block from four different genotype groups, including the control, *Pdk1* cKO, 5×FAD, and *Pdk1* cKO/5×FAD.

2.3. Immunohistochemistry (IHC)

We chose two brain sections, spaced at 400 μm, from each mouse for IHC. The sections were deparaffinized and then rehydrated with degraded ethanol solutions. They were treated with boiled sodium citrate buffer (Xilong Scientific, 160012) for 25 min. The sections were cooled down at room temperature and then blocked with 3% hydrogen peroxide (Sinopharm Chemical Reagent, 10011218) for 20 min. They were subsequently treated with 5% BSA solution (bovine serum albumin dissolved in PBS) (Best Biological, BA0029) for 20 min.

The sections were incubated with primary antibodies at 4°C overnight and then washed out with PBS 3 times before incubation with a secondary antibody at 4°C for 1 h. The DAB Kit (Vector Laboratories, SK-4100) was then used for the processing of the sections. After dehydration, each section was sealed using neutral resin.

All the primary antibodies are listed in Table 1.

For fluorescence IHC, the following secondary antibodies were obtained from Jackson ImmunoResearch Laboratories: Alexa Fluor 488 (715-545-150) and Alexa Fluor 594 (711-585-152). Fluorescence images and IHC images were captured using a confocal microscope from Leica (SP5) and an Olympus microscope (BX53), respectively.

2.4. Western blotting

Cortical tissues were homogenized using cold radioimmunoprecipitation assay (RIPA) buffer to prepare cortical protein lysates[41,42]. The gradients were as follows (in mM): 20 mM tris-hydrochloride (HCl), pH 7.4, 150 mM sodium chloride (NaCl), 1 mM ethylenediaminetetraacetic acid (EDTA), 1% NP-40, 0.5% sodium deoxycholate, and 0.1% sodium dodecyl sulfate (SDS, Yifeixue Biotechnology, YS0005-500). The RIPA lysis buffer contained protease and phosphatase inhibitors. Protein concentration was obtained using a method reported recently[43,44].

Cortical samples were normalized to determine the loading volume for each sample (total proteins = 40 μg). Samples were loaded into 10% SDS-PAGE running gel. Nitrocellulose membranes were used for protein transfer. After the membranes were blocked using a non-fat milk solution (Sangon Biotech, A600669) (5% w/v) for 1 h, they were then probed using the primary antibodies listed in Table 1 at 4°C overnight. The membranes were washed with PBS 3 times (15 min each time) and incubated with the following secondary antibodies: IRdye800 and IRdye680[45,46]. The membranes were scanned using the LI-COR Imaging System.

Table 1. Primary antibodies used for Western blotting and immunohistochemistry.

Antibodies	Suppliers	Catalogue number
Anti-PDK1 antibody	Abcam	ab52893 RRID: AB_881962
Anti-NeuN	Millipore	ABN78 RRID: AB_10807945
Anti-Aβ (1-16) antibody (6E10)	BioLegend	803001 RRID: AB_2564653
Anti-Aβ antibody (D54D2)	Cell Signaling Technology	8243 RRID: AB_2797642
Anti-amyloid precursor protein antibody	Sigma-Aldrich	A8717 RRID: AB_258409
Anti-GFAP antibody	ABclonal	A14673 RRID: AB_2761548
Anti-Iba1 antibody	FUJIFILM Wako Shibayagi	016-20001 RRID: AB_839506
Aniti-phospho-S6 (Ser235/236) antibody	Cell Signaling Technology	2211 RRID: AB_331679
Anti-phospho-4E-BP1 (Ser65) antibody	Cell Signaling Technology	9451 RRID: AB_330947
Anti-BACE1 antibody	Abcam	Ab183612 RRID: N/A
Anti-ADAM10 antibody	Millipore	AB19026 RRID: AB_2242320
Anti-β-actin antibody	GeneTex	4060 RRID: AB_2315049
Anti-GAPDH antibody	CW Biotech	cw0100 RRID: N/A

2.5. Counting methods for cells positive for different markers

For each mouse, we chose two brain sections (spaced 400 μm) to perform IHC for Aβ, glial fibrillary acidic protein (GFAP), or Iba1[37]. First, IHC images for Aβ were taken with the ×10 objective lens in the BX53 microscope, and amyloid plaques (diameter of plaques >5 μm) were counted in each IHC image (an area of 1.364 μm × 1.021 μm). Second, the same microscopy settings were used to capture IHC images for GFAP and Iba1. In each IHC image, GFAP+ cells or Iba1+ cells in the cortex were counted manually.

2.6. Statistical analysis

Data were shown as average ± standard error of mean (SEM). Two-tailed Student's t-test was used to analyze the differences in protein levels, cell numbers, and plaque

numbers between *Pdk1* cKO/5×FAD mice and their 5×FAD littermates. $P < 0.05$ indicated a significant effect.

3. Results

3.1. Molecular analysis of the 5×FAD model with PDK1 deficiency through *Emx1-Cre*-mediated gene recombination

It has been shown that long-term treatment of adult Tg2576 mice with BX912 decreases amyloid plaques but causes lethal effect in mice[22]. To investigate whether the inactivation of PDK1, beginning from the embryonic stage, could prevent AD-like pathology in 5×FAD mice[30], we generated *Pdk1*$^{f/f}$;*Emx1-Cre*/5×FAD (*Pdk1* cKO/5×FAD) mice, in which the deletion of PDK1 begins at embryonic day 10.5 (E10.5) in the forebrain neurons. The four different genotypes are shown in Figure 1A.

To determine the expression pattern of Cre, *Rosa26-LSL-tdTomato* mice[16,47] were crossed to *Emx1-Cre* to generate *Emx1-Cre;Rosa26-LSL-tdTomato*, in which tdTomato is expressed in Cre-positive (Cre+) cells. The brain sections of the double mutant mice at P0 were used to perform costaining for tdTomato and NeuN. We observed abundant tdTomato+/NeuN+ cells in the cortex (Figure 1B). The cell counting results showed that ~92% of NeuN+ cells were positive for tdTomato. Subsequently, we performed fluorescence IHC for PDK1. We found that PDK1 immunoreactivity was qualitatively reduced in the *Pdk1* cKO/5×FAD cortex at 2.5 months compared with 5×FAD littermates (Figure 1C). Western blotting was performed for PDK1 using cortical lysates from mice at 2.5 months. PDK1 levels were notably decreased in the *Pdk1* cKO/5×FAD cortex compared with 5×FAD mice (Figure 1D), suggesting efficient inactivation of PDK1 in *Pdk1* cKO/5×FAD mice.

3.2. Plaque deposition is prevented in 5×FAD mice with PDK1 deficiency

To investigate whether PDK1 deletion affects plaque deposition in 5×FAD mice, IHC was performed for Aβ using brain sections from control, *Pdk1* cKO, 5×FAD, and *Pdk1* cKO/5×FAD mice at three different ages (2.5, 4, and 6 months). First, there were a few amyloid plaques in the 5×FAD cortex at 2.5 months but abundant amyloid plaques at 4 and 6 months compared with non-Tg littermate controls (Figure 2A). In contrast, amyloid plaques were hardly seen in the *Pdk1* cKO/5×FAD cortex at the aforementioned ages

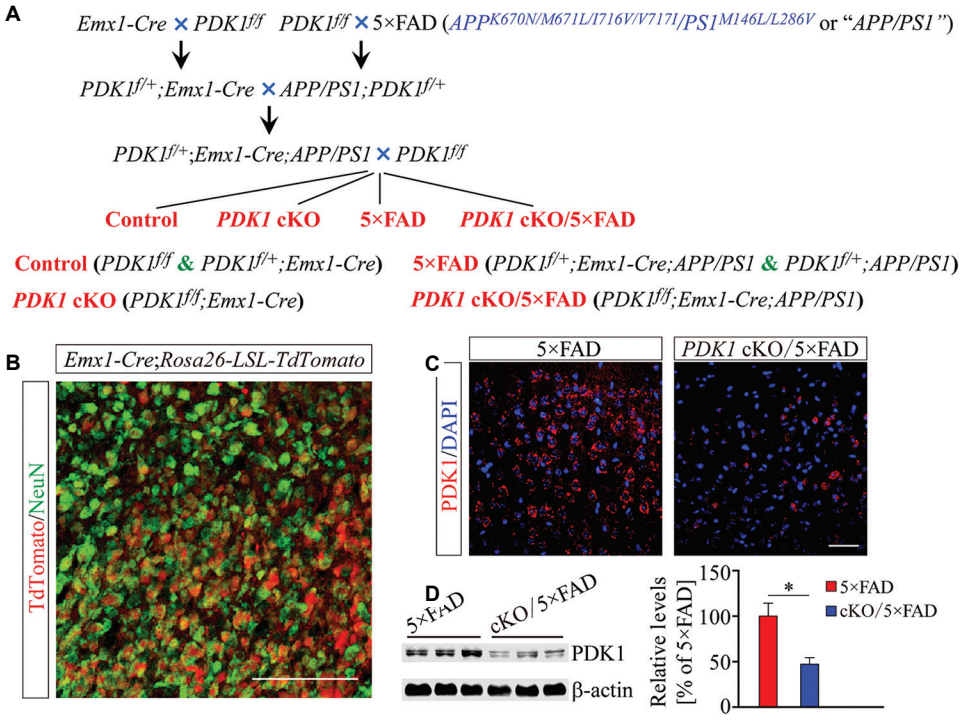

Figure 1. Characterization of forebrain-specific *Pdk1* cKO/5×FAD mice. **(A)** Breeding strategies to generate *Pdk1* cKO/5×FAD mice. *Pdk1*$^{f/f}$ and *Pdk1*$^{f/+}$;*Emx1-Cre* as the control group, *Pdk1*$^{f/f}$;*APP/PS1* and *Pdk1*$^{f/+}$;*Emx1-Cre;APP/PS1* as 5×FAD, *Pdk1*$^{f/f}$;*Emx1-Cre* as *Pdk1* cKO, and *Pdk1*$^{f/f}$;*Emx1-Cre;APP/PS1* as *Pdk1* cKO/5×FAD. **(B)** Representative images of tdTomato/NeuN costaining. Abundant tdTomato+ and tdTomato+/NeuN+ cells were detected in the cortex of *Emx1-Cre;Rosa26-LSL-tdTomato* mice. **(C)** Representative images of fluorescence IHC for PDK1. Sagittal brain sections at 2.5 months were used. The immunoreactivity of PDK1 was qualitatively different between 5×FAD and *Pdk1* cKO/5×FAD mice. The scale bar is 100 μm. **(D)** Western blotting for PDK1. Cortical samples were prepared from 5×FAD and *Pdk1* cKO/5×FAD mice aged at 2.5 months ($n = 3$ mice per group; $^*P < 0.05$).

(Figure 2A and B). Second, quantitative results revealed significant reductions in the average number of plaques in the *Pdk1* cKO/5×FAD cortex at 2.5, 4, and 6 months compared to that in 5×FAD (Figure 2C; $P < 0.001$ at 2.5 months, $P < 0.01$ at 4 months, and $P < 0.001$ at 6 months). Indeed, amyloid plaques were hardly seen in the *Pdk1* cKO/5×FAD cortex (Figure 2A–C). The results suggest that PDK1 deletion may prevent plaque deposition in APP Tg mice.

3.3. Gliosis is alleviated in 5×FAD mice with PDK1 deficiency

Neuroinflammation is a typical feature in mouse models of AD[30,48]. To investigate whether microglia are affected in the *Pdk1* cKO/5×FAD cortex, we performed IHC for Iba1 using brain sections from mice at 2.5, 4, and 6 months. First, Iba1 cortical immunoreactivity did not differ between the control and *Pdk1* cKO mice at each age tested (Figure 3A). However, it was increased in the 5×FAD group at 2.5, 4, and 6 months compared with the control group (Figure 3A and 3B). Second, the average number of Iba1+ cells was significantly higher in the 5×FAD cortex than in the control at 2.5, 4, and 6 months (Figure 3C; $P < 0.001$), but it was significantly lower in the *Pdk1* cKO/5×FAD group at 4 and 6 months compared with the 5×FAD group (Figure 3C; $P < 0.001$). These data suggest that PDK1 deletion may ameliorate microgliosis in APP Tg mice.

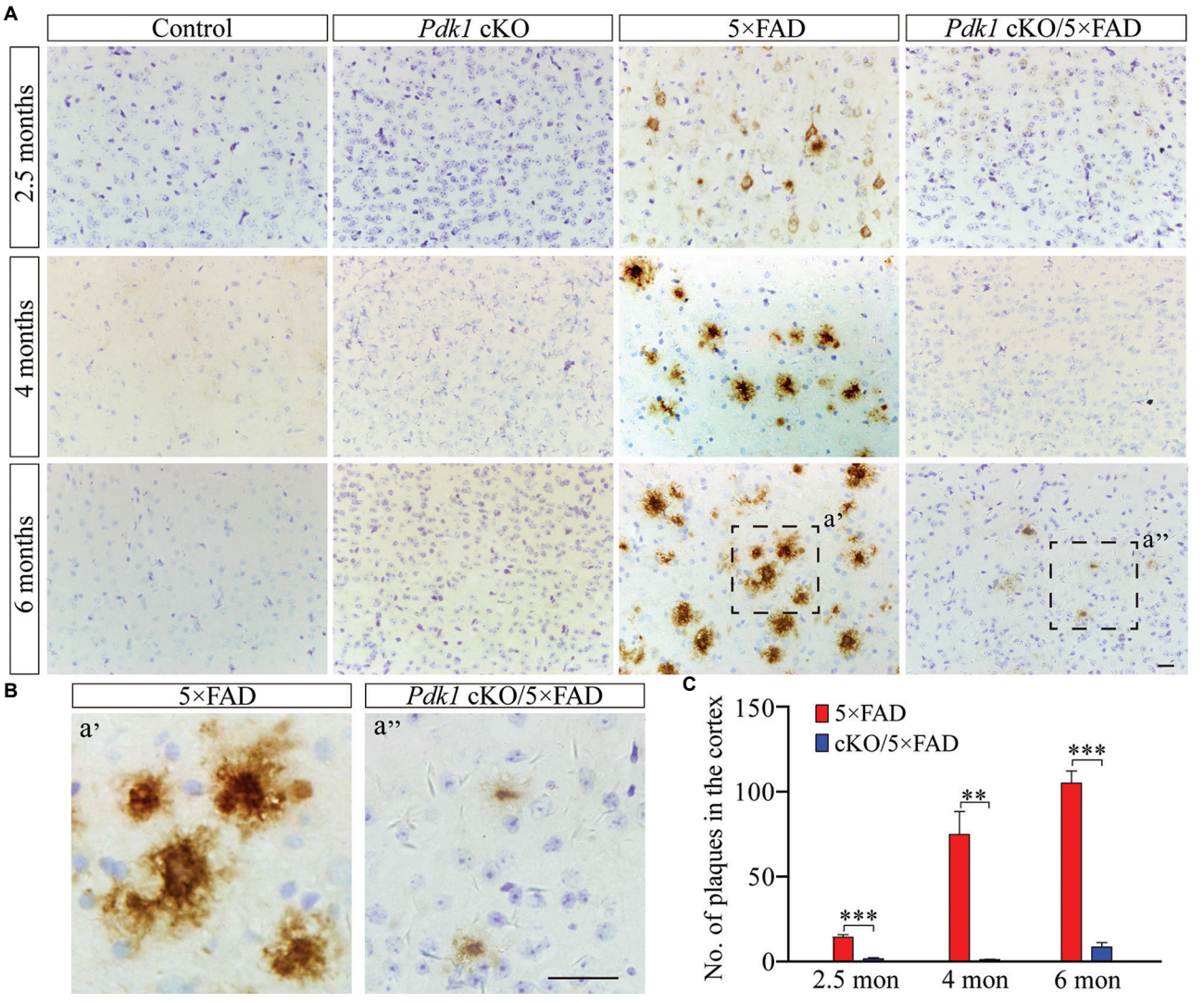

Figure 2. Prevention of Aβ deposition in the cortex of *Pdk1* cKO/5×FAD mice. **(A)** Representative images of Aβ immunostaining. Brain sections at 2.5, 4, and 6 months were used. Images were captured from the cortex of four different groups of mice, including the control, *Pdk1* cKO, 5×FAD, and *Pdk1* cKO/5×FAD groups. The scale bar is 20 μm. **(B)** Enlarged images for boxed regions in **(A)**. The scale bar is 25 μm. **(C)** Quantification results showing the total number of amyloid plaques in the cortex. There were significant differences between 5×FAD and *Pdk1* cKO/5×FAD mice at 2.5 (***$P < 0.001$), 4 (**$P < 0.01$), and 6 months (***$P < 0.001$) (n = 3–5 mice per group per age).

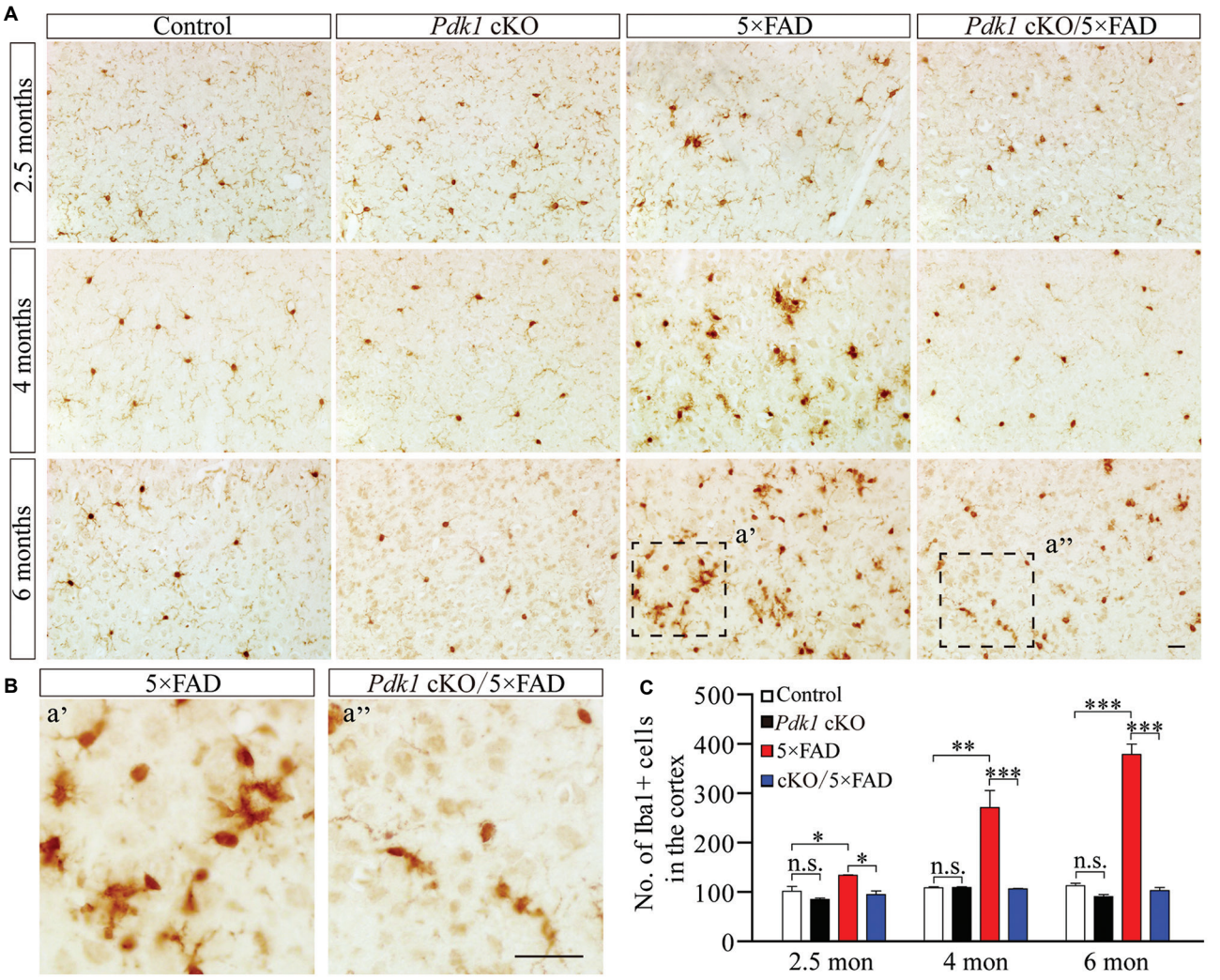

Figure 3. Diminished microgliosis in *Pdk1* cKO/5×FAD mice. **(A)** Representative images of IHC for Iba1 in the cortex. Brain sections were prepared from control, *Pdk1* cKO, 5×FAD, and *Pdk1* cKO/5×FAD mice aged 2.5, 4, and 6 months. The immunoreactivity of Iba1 was qualitatively different between the control and 5×FAD mice. The scale bar is 20 μm. **(B)** Enlarged images for boxed regions in **(A)**. The scale bar is 25 μm. **(C)** Quantification results showing the average number of Iba1+ cells in the cortex. There were significant differences in the number of Iba1+ cells between 5×FAD and *Pdk1* cKO/5×FAD mice at 2.5 (*$P < 0.05$), 4 (***$P < 0.001$), and 6 (***$P < 0.001$) months (n = 3–4 mice per group per age).

To study whether there are changes to astrocytes in *Pdk1* cKO/5×FAD mice, IHC was performed for GFAP. First, it was observed that GFAP immunoreactivity was qualitatively higher in the *Pdk1* cKO cortex and the 5×FAD cortex at 2.5, 4, and 6 months compared with the littermate controls (Figure 4A). GFAP immunoreactivity was reduced in the *Pdk1* cKO/5×FAD cortex compared with the 5×FAD cortex (Figure 4A and B). Second, the total number of GFAP+ cells in the 5×FAD cortex at 4 or 6 months was more than that in the control cortex (Figure 4C; $P < 0.001$), but it was smaller in the *Pdk1* cKO/5×FAD cortex than in the 5×FAD cortex (Figure 4C; $P < 0.001$). These results suggest that astrogliosis may be attenuated by PDK1 deletion in 5×FAD mice.

3.4. mTOR signaling is inhibited in 5×FAD mice with PDK1 deficiency

In the mTOR signaling pathway, S6 kinase (S6K) phosphorylates S6 at Ser235 and Ser236 (Ser235/236) following its activation by mTOR[49,50]. We investigated whether this pathway is affected by PDK1 deletion. First, we performed Western blotting for $pS6^{Ser235/236}$. We found that the levels of $pS6^{Ser235/236}$ were significantly lower in the *Pdk1* cKO/5×FAD cortex than in the 5×FAD cortex (Figure 5A and B). Second, we performed Western blotting for phosphorylated 4E-BP1, an important member of the mTOR pathway[51]. We found that the levels of $p4E\text{-}BP1^{Ser65}$ were lower in the *Pdk1* cKO/5×FAD cortex compared with 5×FAD mice (Figure 5A and B). Third, we performed IHC

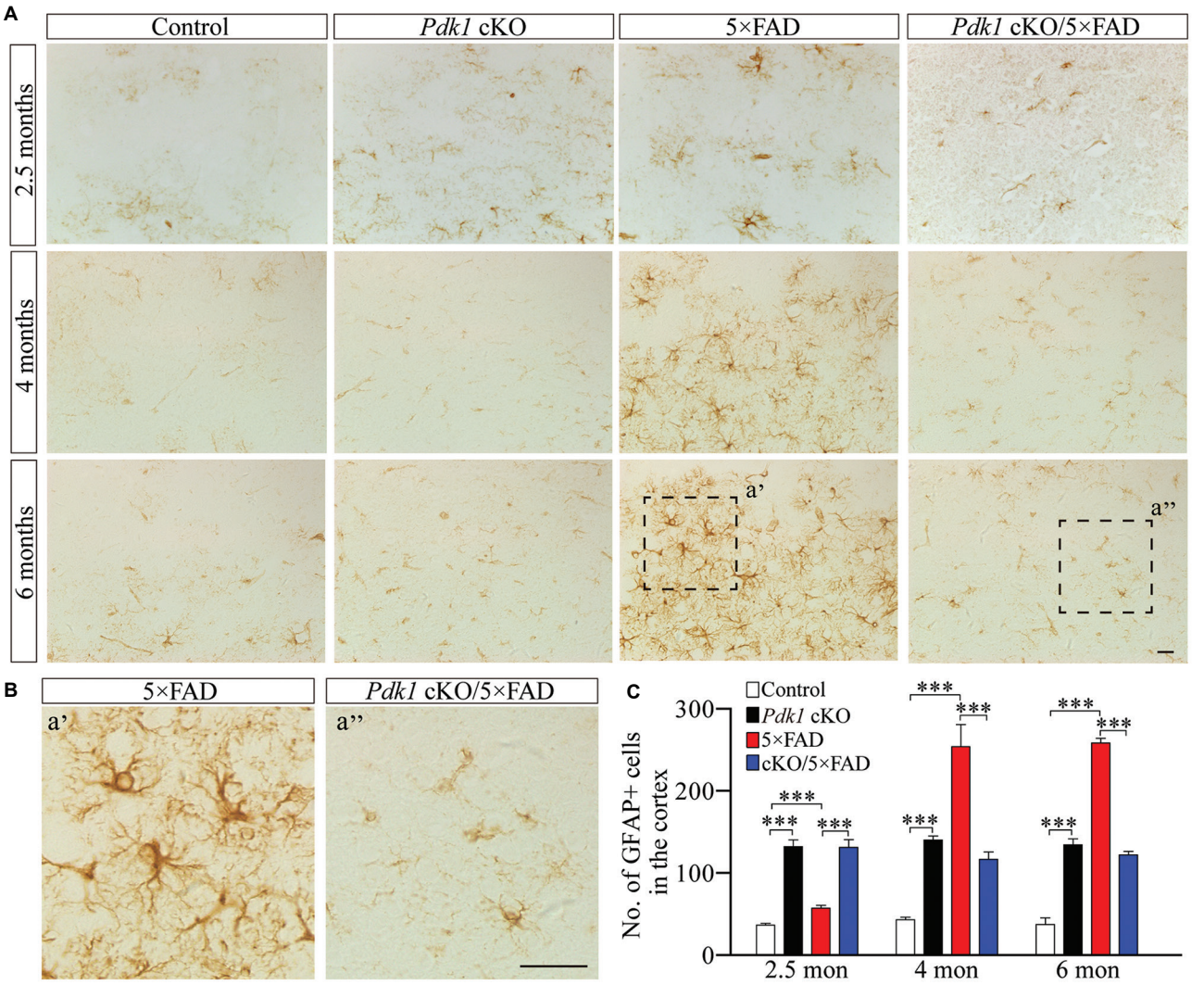

Figure 4. Decreased astrogliosis in *Pdk1* cKO/5×FAD mice. **(A)** Representative images of IHC for GFAP in the cortex. Mice aged at 2.5, 4, and 6 months were used. The immunoreactivity of GFAP was qualitatively increased in 5×FAD mice compared with the controls. The scale bar is 20 μm. **(B)** Enlarged images for boxed regions in **(A)**. The scale bar is 25 μm. **(C)** Quantification results showing the average number of GFAP+ cells in the cortex. There were significant differences in the number of GFAP+ cells between 5×FAD and *Pdk1* cKO/5×FAD mice at 2.5 (***$P < 0.001$), 4 (***$P < 0.001$), and 6 (***$P < 0.001$) months ($n = 3$ mice per group per age).

for pS6$^{Ser235/236}$. Consistent with the biochemical results for pS6, the immunoreactivity of pS6$^{Ser235/236}$ was qualitatively reduced in *Pdk1* cKO/5×FAD mice compared with 5×FAD littermates (Figure 5C). The results are consistent with the notion that PDK1 is an upstream kinase for mTOR[21].

3.5. Expression of APP is decreased in 5×FAD mice with PDK1 deficiency

To determine the molecular mechanisms by which PDK1 deletion reduces Aβ deposition, we focused on APP. Since Aβ is known to be generated from APP through sequential cleavages by β- and γ-secretases[52], Western blotting on APP was performed using cortical samples from four different genotypes of mice (Figure 6A). Total APP levels were robustly higher in the 5×FAD cortex than in the control cortex (Figure 6B) and significantly lower in *Pdk1* cKO/5×FAD mice than in 5×FAD mice (Figure 6B). Next, IHC for APP was performed. The results showed that APP immunoreactivity was qualitatively reduced in *Pdk1* cKO/5×FAD mice than in 5×FAD mice (Figure 6C).

We also performed Western blotting to examine the products of APP cleaved by α- and γ-secretases: Secreted (s)APPα and APP-C-terminal fragment (CTF) (Figure 6D). Our results revealed that protein levels for sAPPα and APP-CTF were significantly lower in *Pdk1* cKO/5×FAD mice than in 5×FAD mice

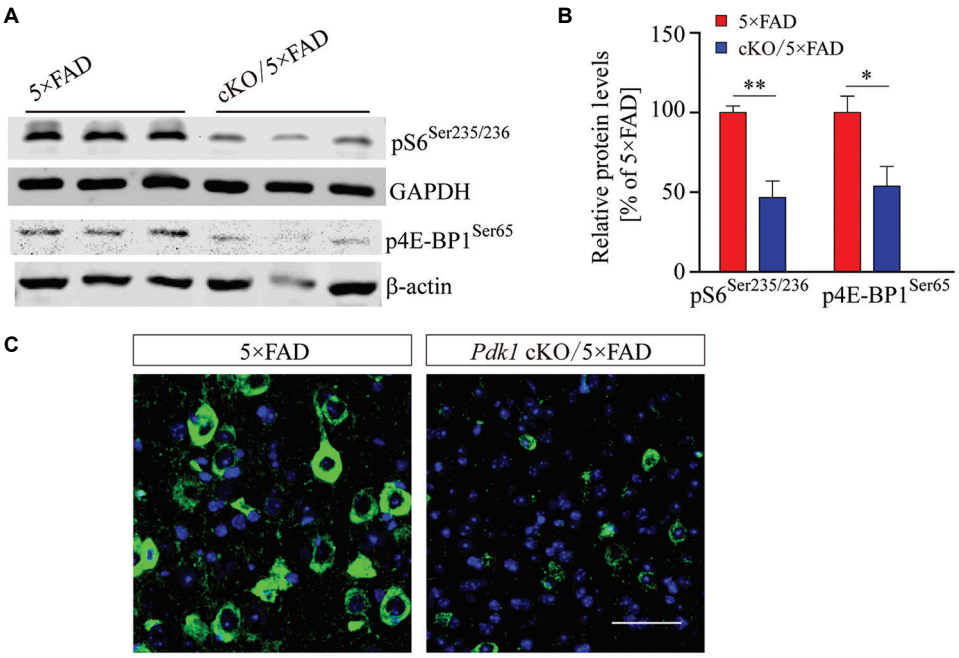

Figure 5. Reduced mTOR activity in *Pdk1* cKO/5×FAD mice. **(A and B)** Western blotting for $pS6^{Ser235/236}$ and $p4E\text{-}BP1^{Ser65}$. **(A)** Cortical samples from 5×FAD and *Pdk1* cKO/5×FAD mice were used. **(B)** There were significant differences in the relative levels of $pS6^{Ser235/236}$ and $p4E\text{-}BP1^{Ser65}$ between 5×FAD and *Pdk1* cKO/5×FAD mice at 4 months (n = 3–4 mice per group; $^{*}P < 0.05$, $^{**}P < 0.01$). **(C)** Fluorescence IHC for $pS6^{Ser235/236}$. Brain sections at 4 months were used. The immunoreactivity of $pS6^{Ser235/236}$ was qualitatively different between 5×FAD and *Pdk1* cKO/5×FAD mice. The scale bar is 50 μm.

(Figure 6D and 6E). These findings are consistent with those for total APP (Figure 6A). Moreover, we found that the ratio of sAPPα to total APP was similar between 5×FAD and *Pdk1* cKO/5×FAD mice (Figure 6F). Since α- and β-secretases are responsible for Aβ generation[53], we performed Western blotting for a disintegrin and metalloproteinase 10 (ADAM10) and beta-site APP cleaving enzyme 1 (BACE1). However, the levels of these two proteins did not significantly differ in 5×FAD and *Pdk1* cKO/5×FAD mice (Figure 6G and H).

4. Discussion

The recent study by Petri *et al.* suggests that pharmacological inhibition on PDK1 may be beneficial to AD. The aim of this study was to test whether early inhibition of PDK1 may prevent AD-like pathology in APP Tg mice. In this study, *Emx1-Cre*-mediated *Pdk1* cKO/5×FAD mice were used. We demonstrated that PDK1 deletion prevents plaque deposition and attenuates gliosis in the 5×FAD cortex. In addition, PDK1 deletion inhibits the mTOR signaling pathway and downregulates APP expression in 5×FAD mice. Overall, these findings are consistent with the notion that PDK1 could be a promising therapeutic target for AD.

As previously reported, long-term treatment with BX912 results in the death of Tg2576 mice[22]. In line with this, straight KO of *Pdk1* leads to early embryonic lethality in mice[27]. In contrast, *Emx1-Cre*-mediated PDK1 deletion does not cause any lethal effect in mice. We did not observe any abnormal deaths in *Pdk1* cKO/5×FAD mice or in *Pdk1* cKO mice. Nevertheless, the pharmacological method[22] and genetic approach used in the present study may efficiently inhibit PDK1 function. However, it is known that *Emx1-Cre*-mediated PDK1 deletion disrupts the formation of cortex in mice[28]. Therefore, we cannot exclude the possibility that a reduced cortex size may play a role in improving AD-like pathology in *Pdk1* cKO/5×FAD mice.

Genetic approaches have been widely used in neurodegenerative diseases[54]. First, a gene therapy-based clinical trial has revealed high treatment efficacy in spinal muscular atrophy (SMA) type 1[55]. Second, genetic approaches have been tested in animal models for amyotrophic lateral sclerosis[56] and Huntington's disease[57]. Third, the CRISPR-Cas9 technology was employed in a study to inactivate the mutant human *APP* gene in 5×FAD mice, resulting in a significant alleviation of AD-like pathology[58]. Based on our finding that early inhibition of PDK1 prevents AD-like pathology in 5×FAD mice, we propose the development of a genetic approach that targets neuronal PDK1 as a potential treatment strategy for AD.

To identify the underlying molecular mechanisms in *Pdk1* cKO/5×FAD mice, we examined the expression of APP and APP processing enzymes, including α-secretase

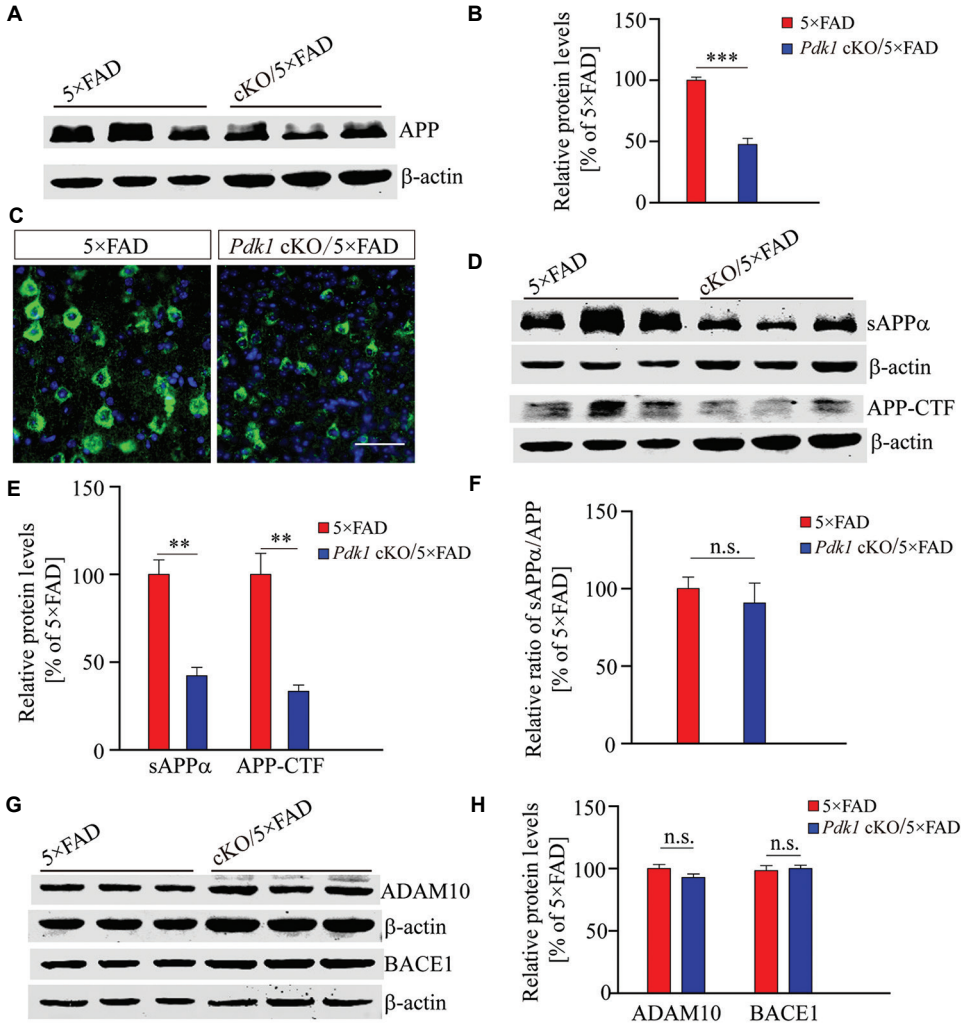

Figure 6. Reduced amyloid precursor protein (APP) expression in *Pdk1* cKO/5×FAD mice. **(A)** Western blotting for full-length APP (APP-FL). Cortical samples from 5×FAD and *Pdk1* cKO/5×FAD mice were used. β-actin was used as the loading control. **(B)** Quantification results of APP-FL. There was a significant difference in the APP levels between 5×FAD and *Pdk1* cKO/5×FAD mice ($n = 3$ mice per group; $^{***}P < 0.001$). **(C)** Fluorescence IHC for APP. Brain sections at 4 months were used. The immunoreactivity of APP was qualitatively reduced in *Pdk1* cKO/5×FAD mice compared with 5×FAD mice. The scale bar is 50 μm. **(D)** Western blotting for sAPPα and APP-CTF. Cortical samples from 5×FAD and *Pdk1* cKO/5×FAD mice at 4 months were used. β-actin served as the loading control. **(E)** Quantification results of sAPPα and APP-CTF. There were significant differences in the levels of sAPPα and APP-CTF between 5×FAD and *Pdk1* cKO/5×FAD mice ($^{**}P < 0.01$; $n = 3$ mice per group). **(F)** Quantification results showing the ratio of sAPPα to APP. There was no significant difference between 5×FAD and *Pdk1* cKO/5×FAD mice (n.s., not significant; $n = 3$ mice per group). **(G)** Western blotting for ADAM10 and BACE1. β-actin was used as the loading control. **(H)** Quantification results of ADAM10 and BACE1. There were no significant differences in the levels of ADAM10 and BACE1 between 5×FAD and *Pdk1* cKO/5×FAD mice (n.s., not significant; $n = 3$ mice per group).

and BACE1. Since the levels of APP were significantly reduced in the *Pdk1* cKO/5×FAD cortex, we reason that this may be responsible for the prevention of plaque deposition. In agreement with this, Duan *et al.* have reported that CRISPR-Cas9-mediated KO of mutant human *APP* gene reduces amyloid plaques and improves spatial working memory in 5×FAD mice.

On the other hand, no changes have been observed in the levels of ADAM10, BACE1, and sAPPα in *Pdk1* cKO/5×FAD cortices, suggesting a possibility that PDK1 deletion may not enhance the activity of α-secretase or β-secretase. In contrast, evidence has shown that BX912 may promote α-secretase-dependent cleavage of APP[22]. We reason that the above discrepancy reflects the fact that pharmacological and genetic approaches exhibit different target selectivity and cell specificity[37]. For instance, BX912 is known to inhibit a spectrum of kinases, including PDK1[59,60]. In contrast, *Emx1-Cre*-mediated gene recombination permits conditional inactivation of PDK1 in neurons in the postnatal forebrain.

Since ribosomal kinase S6 is a key member of the mTOR signaling pathway[15,16,21], the decreased pS6 levels suggest that the activity of mTOR may be reduced in the *Pdk1* cKO/5×FAD cortex. Since previous evidence has shown that S6 is essential for ribosome biogenesis[61], it is likely that ribosome biogenesis may be regulated by PDK1 via S6[37]. In essence, the following molecular and cellular mechanisms may be responsible for the prevention effects on AD-like pathology as observed in *Pdk1* cKO/5×FAD mice. First, PDK1 deletion causes a reduction in mTOR signaling and subsequently inhibits the activity of S6. Second, the deactivation of S6 may impair ribosome-dependent protein synthesis, which then downregulates APP expression at the translational level[37]. Third, Aβ generation from APP is repressed, and gliosis is ameliorated in the forebrain of *Pdk1* cKO/5×FAD mice.

5. Conclusion

Deletion of PDK1 in the developing cortex prevents plaque deposition and ameliorates gliosis in 5×FAD mice. PDK1 deletion inhibits mTOR signaling activity and downregulates APP expression. PDK1 may serve as a potential target for the treatment of AD.

Acknowledgments

We thank Xiaochuan Zou for technical assistance.

Funding

This study was partially supported by the National Natural Science Foundation of China (NSFC91849113), the Natural Key Research and Development Program of China (2022ZD0211803), the Natural Science Foundation of Jiangsu (BK20201255), and the Changzhou Municipal Key Research Program (CJ20210112).

Conflict of interest

The authors have no conflicts of interest to declare.

Author contributions

Conceptualization: Yimin Hu, Bing Zhang, and Guiquan Chen

Formal analysis: Xiaolian Ye, Liyang Yao, Wenhao Chen, and Wenkai Shao

Investigation: Xiaolian Ye, Liyang Yao, Wenhao Chen, and Wenkai Shao

Methodology: Xiaolian Ye, Liyang Yao, Wenhao Chen, and Wenkai Shao

Writing – original draft: Xiaolian Ye and Guiquan Chen

Writing – review & editing: Guiquan Chen

Ethics approval and consent to participate

An animal protocol (AP) for this study was approved by the Institutional Animal Care and Use Committee (IACUC) of the MARC at Nanjing University.

Consent for publication

Not applicable.

Availability of data

The experimental materials used in this study are available from corresponding authors on reasonable request.

References

1. Li T, Han Y, 2022, Insights on amyloid-related imaging abnormalities from the "Pre-Alzheimer's Disease Alliance of China". *Adv Neurol*, 1: 2.
2. Scheltens P, Blennow K, Breteler MM, *et al.*, 2016, Alzheimer's disease. *Lancet*, 388: 505–517.
3. Horsburgh K, Holland P, Reimer M, *et al.*, 2011, Axon-glial disruption: The link between vascular disease and Alzheimer's disease? *Biochem Soc Trans*, 39: 881–885.
4. Frisoni GB, Altomare D, Thal DR, *et al.*, 2022, The probabilistic model of Alzheimer disease: The amyloid hypothesis revised. *Nat Rev Neurosci*, 23: 53–66.
5. Hardy, J, Selkoe DJ, 2002, The amyloid hypothesis of Alzheimer's disease: Progress and problems on the road to therapeutics. *Science*, 297: 353–356.
6. Goedert M, Eisenberg DS, Crowther RA, 2017, Propagation of Tau aggregates and neurodegeneration. *Ann Rev Neurosci*, 40: 189–210.
7. Mintun MA, Lo AC, Evans CD, *et al.*, 2021, Donanemab in early Alzheimer's disease. *N Engl J Med*, 384: 1691–1704.
8. Sevigny J, Chiao P, Bussiere T, *et al.*, 2016, The antibody aducanumab reduces A beta plaques in Alzheimer's disease. *Nature*, 537: 50–56.
9. Peng Y, Hu Y, Xu S, *et al.*, 2012, L-3-n-butylphthalide reduces tau phosphorylation and improves cognitive deficits in AbetaPP/PS1-Alzheimer's transgenic mice. *J Alzheimers Dis*, 29: 379–391.
10. Peng Y, Sun J, Hon S, *et al.*, 2010, L-3-n-butylphthalide improves cognitive impairment and reduces amyloid-beta in a transgenic model of Alzheimer's disease. *J Neurosci*, 30: 8180–8189.
11. Chen G, Chen KS, Kobayashi D, *et al.*, 2007, Active-amyloid immunization restores spatial learning in PDAPP mice displaying very low levels of beta-amyloid. *J Neurosci*, 27: 2654–2662.
12. Schenk D, Barbour R, Dunn W, *et al.*, 1999, Immunization with amyloid-attenuates Alzheimer-disease-like pathology in the PDAPP mouse. *Nature*, 400: 173–177.

13. Yao YL, Wang YX, Yang FC, *et al.*, 2022, Targeting AKT and CK2 represents a novel therapeutic strategy for SMO constitutive activation-driven medulloblastoma. *CNS Neurosci Ther*, 28: 1033–1044.

14. Wang J, Yu Z, Tao Y, *et al.*, 2021, A novel palmitic acid hydroxy stearic acid (5-PAHSA) plays a neuroprotective role by inhibiting phosphorylation of the m-TOR-ULK1 pathway and regulating autophagy. *CNS Neurosci Ther*, 27: 484–496.

15. Wang H, Liu M, Zou G, *et al.*, 2021, Deletion of PDK1 in oligodendrocyte lineage cells causes white matter abnormality and myelination defect in the central nervous system. *Neurobiol Dis*, 148: 105212.

16. Wang H, Liu M, Ye Z, *et al.*, 2021, Akt regulates Sox10 expression to control oligodendrocyte differentiation via phosphorylating FoxO1. *J Neurosci*, 41: 8163–8180.

17. Ma Y, Xu X, Li C, *et al.*, 2021, Induced neural progenitor cell-derived extracellular vesicles promote neural progenitor cell survival via extracellular signal-regulated kinase pathway. *CNS Neurosci Ther*, 27: 1605–1609.

18. Fedder-Semmes KN, Appel B, 2021, The Akt-mTOR pathway drives myelin sheath growth by regulating Cap-dependent translation. *J Neurosci*, 41: 8532.

19. Bonet IJ, Khomula EV, Araldi D, *et al.*, 2021, PI3K/AKT signaling in high molecular weight hyaluronan (HMWH)-induced anti-hyperalgesia and reversal of nociceptor sensitization. *J Neurosci*, 41: 8414.

20. Zhao XF, Liao Y, Alam MM, *et al.*, 2020, Microglial mTOR is neuronal protective and antiepileptogenic in the pilocarpine model of temporal lobe epilepsy. *J Neurosci*, 40: 7593.

21. Fruman DA, Chiu H, Hopkins BD, *et al.*, 2017, The PI3K pathway in human disease. *Cell*, 170: 605–635.

22. Pietri M, Dakowski C, Hannaoui S, *et al.*, 2013, PDK1 decreases TACE-mediated alpha-secretase activity and promotes disease progression in prion and Alzheimer's diseases. *Nat Med*, 19: 1124–1131.

23. Pei JJ, Khatoon S, An WL, *et al.*, 2003, Role of protein kinase B in Alzheimer's neurofibrillary pathology. *Acta Neuropathol*, 105: 381–392.

24. Mathys H, Davila-Velderrain J, Peng Z, *et al.*, 2019, Single-cell transcriptomic analysis of Alzheimer's disease. *Nature*, 570: 332–337.

25. Yang S, Pascual-Guiral S, Ponce R, *et al.*, 2018, Reducing the levels of Akt activation by PDK1 knock-in mutation protects neuronal cultures against synthetic smyloid-beta peptides. *Front Aging Neurosci*, 9, 435.

26. Stein TD, Johnson, JA, 2002, Lack of neurodegeneration in transgenic mice overexpressing mutant amyloid precursor protein is associated with increased levels of transthyretin and the activation of cell survival pathways. *J Neurosci*, 22: 7380.

27. Lawlor MA, Mora A, Ashby PR, *et al.*, 2002, Essential role of PDK1 in regulating cell size and development in mice. *EMBO J*, 21: 3728–3738.

28. Xu C, Yu L, Hou J, *et al.*, 2017, Conditional deletion of PDK1 in the forebrain causes neuron loss and increased apoptosis during cortical development. *Front Cell Neurosci*, 11: 330.

29. Wei YJ, Han XN, Zhao CJ, 2020, PDK1 regulates the survival of the developing cortical interneurons. *Mol Brain*, 13: 65.

30. Oakley H, Cole SL, Logan S, *et al.*, 2006, Intraneuronal-amyloid aggregates, neurodegeneration, and neuron loss in transgenic mice with five familial Alzheimer's disease mutations: Potential factors in amyloid plaque formation. *J Neurosci*, 26: 10129–10140.

31. Liu T, Zhu X, Huang C, *et al.*, 2022, ERK inhibition reduces neuronal death and ameliorates inflammatory responses in forebrain-specific *Ppp2cα* knockout mice. *FASEB J*, e222515.

32. Huang C, Liu T, Wang Q, *et al.*, 2020, Loss of PP2A disrupts the retention of radial glial progenitors in the telencephalic niche to impair the generation for late-born neurons during cortical development. *Cereb Cortex*, 30: 4183–4196.

33. Cheng S, Liu T, Hu, Y, *et al.*, 2019, Conditional inactivation of Pen-2 in the developing neocortex leads to rapid switch of apical progenitors to basal progenitors. *J Neurosci*, 39: 2195–2207.

34. Englund C, Fink A, Lau C, *et al.*, 2005, Pax6, Tbr2, and Tbr1 are expressed sequentially by radial glia, intermediate progenitor cells, and postmitotic neurons in developing neocortex. *J Neurosci*, 25: 247–251.

35. Wu J, Shao C, Ye X, *et al.*, 2021, *In vivo* brain imaging of amyloid-aggregates in Alzheimer's disease with a near-infrared fluorescent probe. *ACS Sensors*, 6: 863–870.

36. Ma X, Wang Y, Hua J, *et al.*, 2020, Abeta-sheet-targeted theranostic agent for diagnosing and preventing aggregation of pathogenic peptides in Alzheimer's disease. *Sci CHINA Chem*, 63: 73–82.

37. Ye X, Chen L, Wang H, *et al.*, 2022, Genetic inhibition of PDK1 robustly reduces plaque deposition and ameliorates gliosis in the 5×FAD mouse model of Alzheimer's disease. *Neuropathol Appl Neurobiol*, 48: e12839.

38. Han X, Wei Y, Ba R, *et al.*, 2021, PDK1 regulates the lengthening of G1 phase to balance RGC proliferation and differentiation during cortical neurogenesis. *Cereb Cortex*, 32: 3488–3500.

39. Han X, Wei Y, Wu X, *et al.*, 2020, PDK1 regulates transition period of apical progenitors to basal progenitors by controlling asymmetric cell division. *Cereb Cortex*, 30: 406–420.

40. Wang L, Cheng S, Yin Z, *et al.*, 2015, Conditional inactivation of Akt three isoforms causes tau hyperphosphorylation in the brain. *Mol Neurodegener*, 10: 33.

41. Li QQ, Chen J, Hu P, *et al.*, 2022, Enhancing GluN2A-type NMDA receptors impairs long-term synaptic plasticity and

learning and memory. *Mol Psychiatry*: s41380-022-01579-7.

42. Peng SX, Wang YY, Zhang M, *et al.*, 2021, SNP rs10420324 in the AMPA receptor auxiliary subunit TARP γ-8 regulates the susceptibility to antisocial personality disorder. *Sci Rep*, 11: 11997.

43. Xia Y, Zhang Y, Xu M, *et al.*, 2022, Presenilin enhancer2 is crucial for the transition of apical progenitors into neurons but into not basal progenitors in the developing hippocampus. *Development*, 149: dev200272.

44. Teng X, Hu P, Chen Y, *et al.*, 2022, A novel Lgi1 mutation causes white matter abnormalities and impairs motor coordination in mice. *FASEB J*, 36: e22212.

45. Hou J, Bi H, Ye Z, *et al.*, 2021, Pen-2 negatively regulates the differentiation of oligodendrocyte precursor cells into astrocytes in the central nervous system. *J Neurosci*, 41: 4976–4990.

46. Bi H, Zhou C, Zhang Y, *et al.*, 2021, Neuron-specific deletion of presenilin enhancer2 causes progressive astrogliosis and age-related neurodegeneration in the cortex independent of the Notch signaling. *CNS Neurosci Ther*, 27: 174–185.

47. Hou J, Bi H, Ge Q, *et al.*, 2022, Heterogeneity analysis of astrocytes following spinal cord injury at single-cell resolution. *FASEB J*, 36: e22442.

48. Saura CA, Chen G, Malkani S, *et al.*, 2005, Conditional inactivation of presenilin 1 prevents amyloid accumulation and temporarily rescues contextual and spatial working memory impairments in amyloid precursor protein transgenic mice. *J Neurosci*, 25: 6755–6764.

49. Lai KO, Liang ZY, Fei EK, *et al.*, 2015, Cyclin-dependent kinase 5 (Cdk5)-dependent phosphorylation of p70 ribosomal S6 kinase 1 (S6K) is required for dendritic spine morphogenesis. *J Biol Chem*, 290: 14637–14646.

50. Ruvinsky I, Meyuhas O, 2006, Ribosomal protein S6 phosphorylation: From protein synthesis to cell size. *Trends Biochem Sci*, 31: 342–348.

51. Hay N, Sonenberg N, 2004, Upstream and downstream of mTOR. *Genes Dev*, 18: 1926–1945.

52. Kimberly WT, LaVoie MJ, Ostaszewski BL, *et al.*, 2003, Gamma-secretase is a membrane protein complex comprised of presenilin, nicastrin, Aph-1, and Pen-2. *Proc Natl Acad Sci USA*, 100: 6382–6387.

53. De Strooper B, Karran E, 2016, The cellular phase of Alzheimer's disease. *Cell*, 164: 603–615.

54. Anguela XM, High KA, 2019, Entering the modern era of gene therapy. *Ann Rev Med*, 70: 273–288.

55. Mendell JR, Al-Zaidy S, Shell R, *et al.*, 2017, Single-dose gene-replacement therapy for spinal muscular atrophy. *N Engl J Med*, 377: 1713–1722.

56. Thomsen GM, Gowing G, Latter J, *et al.*, 2014, Delayed disease onset and extended survival in the SOD1G93A rat model of amyotrophic lateral sclerosis after suppression of mutant SOD1 in the motor cortex. *J Neurosci*, 34: 15587.

57. McBride JL, Pitzer MR, Boudreau RL, *et al.*, 2011, Preclinical safety of RNAi-mediated HTT suppression in the rhesus macaque as a potential therapy for Huntington's disease. *Mol Ther*, 19: 2152–2162.

58. Duan YY, Ye T, Qu Z, *et al.*, 2022, Brain-wide Cas9-mediated cleavage of a gene causing familial Alzheimer's disease alleviates amyloid-related pathologies in mice. *Nat Biomed Eng*, 6: 168–180.

59. Peifer C, Alessi DR, 2008, Small molecule inhibitors of PDK1. *ChemMedChem*, 3: 1810–1838.

60. Bain J, Plater L, Elliott M, *et al.*, 2007, The selectivity of protein kinase inhibitors: A further update. *Biochem J*, 408: 297–315.

61. Pelletier J, Thomas G, Volarević S, 2018, Ribosome biogenesis in cancer: New players and therapeutic avenues. *Nat Rev Cancer*, 18: 51–63.